# Hemorrhagic Toxins From Rattlesnake (*Crotalus atrox*) Venom

## *Pathogenesis of Hemorrhage Induced by Three Purified Toxins*

Charlotte L. Ownby, PhD, Jón Bjarnason, PhD, and Anthony T. Tu, PhD

**The pathogenesis of hemorrhage induced by three purified components of rattlesnake (*Crotalus atrox*) venom was studied at the light and electron microscopic levels. Crude venom was fractionated by anion exchange and gel filtration in four steps. β-Alanine acetate disk gel electrophoresis was used to demonstrate electrophoretic homogeneity. White mice were injected intramuscularly with 0.1 ml of a sublethal dose of hemorrhagic toxin. Gross examination revealed extensive hemorrhage 5 minutes after the injection of hemorrhagic toxins *a* and *e*; the same amount of hemorrhage was not present until 3 hours after the injection of hemorrhagic toxin *b*. Light microscopic examination of muscle after injection of the toxins revealed areas of extensive hemorrhage in which very few intact capillaries could be found and also adjacent areas of slight hemorrhage in which capillaries were in various stages of degeneration. Necrosis of muscle cells was evident in tissue injected with hemorrhagic toxin *b*. Electron microscopic examination showed that capillaries from toxin-injected muscle were in various stages of degeneration. Endothelial cells became very thin and broke down into vesicles prior to complete rupture. Gaps were formed within the cells while intercellular junctions remained intact. Plasma and erythrocytes leaked through these gaps and were observed in the endomysium. Many gaps were plugged with platelet aggregations. Collagen and the basal lamina associated with capillaries were usually disorganized or absent. The experimental injection of three purified hemorrhagic toxins induced hemorrhage by the same mechanism as does the crude venom, ie, per rhexis. In addition, one of the toxins, hemorrhagic toxin *b*, causes myonecrosis. (Am J Pathol 93:201–218, 1978)**

RATTLESNAKE ENVENOMATION results in hemorrhage and myonecrosis, which are usually not prevented by treatment with commercially available antivenin. The pathogenesis of hemorrhage [1] and myonecrosis [2] induced by crude rattlesnake venom has been studied. Cameron and Tu [3] isolated in pure form a mytoxic component from the venom of the Prairie rattlesnake (*Crotalus viridis viridis*), and Ownby et al [4] described the pathogenesis of myonecrosis induced by the pure toxin myotoxin *a*.

---

From the Department of Physiological Science, Oklahoma State University, Stillwater, Oklahoma, and the Department of Biochemistry, Colorado State University, Fort Collins, Colorado.

Supported by the Department of Physiological Sciences, College of Veterinary Medicine and the Presidential Challenge Grant Program, Oklahoma State University (Dr. Ownby) and by Grant R01 GM 15591 (Dr. Tu).

Accepted for publication June 12, 1978.

Address reprint requests to Anthony T. Tu, PhD, Department of Biochemistry, Colorado State University, Fort Collins, CO 80523.

0002-9440/78/1010-0201$01.00

Numerous attempts have been made to isolate and characterize hemorrhagic components from snake venom, but little has been done to further our understanding of their biologic modes of action. Three hemorrhagic components (HR-1, HR-2a, and HR-2b) have been isolated from the venom of *Trimeresurus flavoviridis*.[5-7]

Two hemorrhagic components (HRI and HRII) have been isolated from the venom of *Agkistrodon halys blomhoffii* [8-10] but the pathogenesis of hemorrhage induced by them has not been studied.

One hemorrhagic component was isolated from *Vipera palestinae* venom [11] and one from *Bothrops jararaca* venom.[12] Recently, a proteinase was isolated from *A acutus* venom which was shown to cause hemorrhage.[13] Bjarnason and Tu [14] isolated five hemorrhagic components from rattlesnake (*C atrox*) venom and named them hemorrhagic toxins *a*, *b*, *c*, *d*, and *e*.

Although hemorrhagic toxins have been isolated and chemically characterized, there has been little work done on their biologic modes of action. As a result, little is known about the pathogenesis of hemorrhage induced by pure hemorrhagic toxins. Several studies of snake-venom–induced hemorrhage have been made using crude venoms.

We investigated the pathogenesis of hemorrhage induced by the crude venom of *C atrox* and found a direct lytic action on endothelial cells which resulted in hemorrhage by rhexis.[1] Sandbank et al [15] studied the effects of *Echis coloratus* venom on brain capillaries. Leakage of an electron-dense tracer was by two mechanisms: endothelial cell pinocytosis and opening of intercellular junctions. McKay et al [16] noted a direct lytic action of a purified hemorrhagin from *V palestinae* venom on capillary endothelium. They noted swollen endothelial cells, platelet aggregations, intact intercellular junctions, complete necrosis of endothelial cells, and the escape of erythrocytes through gaps in damaged endothelial cells.

Cinematographic [17] and electron microscopic [18] examination of hemorrhage induced by Habu (*T flavoviridis*) venom and its main hemorrhagic principle, HR-1, indicates that erythrocytes escape through widened intercellular junctions. Lysis of endothelial cells apparently does not occur. Ohsaka et al [19] reported that the purified hemorrhagic components release proteins and carbohydrates from isolated basement membranes and concluded that this action was the basis for their hemorrhagic effect.

Our studies of the pathogenesis of hemorrhage induced by crude *C atrox* venom [1] indicate that this venom exerts a direct effect on capillary endothelial cells, producing dilatation of endoplasmic reticulum, swollen cytoplasm, blebbing, and, eventually, rupture of the plasma membrane followed by extravasation of blood. We did not observe hemorrhage per diapedesis following injection of crude *C atrox* venom.

The purpose of this investigation was to determine the pathogenesis of hemorrhage induced by injection of each of three pure hemorrhagic toxins isolated from *C atrox* venom and to compare the mechanisms by which the three toxins induce hemorrhage with mechanisms of pure toxins and of crude venom.

## Materials and Methods

### Fractionation of Venom

Crude western diamondback rattlesnake (*C atrox*) venom in lyophilized form was purchased from Miami Serpentarium Laboratories. Two samples of crude venom (10 g each) were dissolved in 50 ml distilled water and dialyzed against four changes (1 liter each) of 10 mM borate containing 0.1 M NaCl and 2 mM $CaCl_2$ (pH 9.0 at 22 C). Each sample was applied to a Whatman DE 32 anion exchange column (2.5 × 35 cm) equilibrated with the borate buffer. A two-step elution was used to develop the column: first with 1000 ml of the starting buffer then with the same buffer containing 0.4 M NaCl and 2 mM $CaCl_2$. Eluate absorbance at 280 nm was monitored with a Beckman DG-B spectrometer. The amount of protein was determined by the Hartree modification of the Lowry method [20] using bovine serum albumin as a protein standard.

Fractions A-1, A-2, and A-4 from the anion exhange column were further fractionated by one of three procedures.[14,21] Briefly, fraction A-1 was further separated using Sephadex G-75, Whatman DE32, CM32, and Ultragel AcA44 columns to give hemorrhagic toxins *a* and *b*. Fraction A-2 was further separated using Whatman DE32 columns into hemorrhagic toxins *c* and *d*, and fraction A-4 was separated on Sephadex G-75 and Whatman DE32 columns to yield hemorrhagic toxin *e*.

### Assay for Hemorrhagic Activity During Fractionation

Swiss Webster white mice weighing 20 g were used for assay of hemorrhagic activity. They were injected subcutaneously with a solution containing approximately 10 $\mu$g protein in 0.1 ml 0.9% NaCl. After 6 hours the mice were killed by cervical dislocation; a dorsal patch of skin was removed and the inside surface was observed for hemorrhage. If the area of hemorrhage resulting from injection of a fraction was equal to or larger than that caused by an equal amount of crude venom, the fraction was designated hemorrhagic. Determination of the minimum hemorrhagic dose of crude venom and purified fractions was done using Kondo's procedure [22] with the following modifications. Five Swiss Webster white mice (20 g) were injected with each dose and killed after 6 hours. The minimum hemorrhagic dose was defined as the lowest dose which caused an area of hemorrhage of 5 mm in diameter 6 hours after subcutaneous injection.[14]

### Demonstration of Protein Homogeneity

Disk gel electrophoresis was done using the $\beta$-alanine acetate disk gel system and the results were reported by Bjarnason and Tu.[14]

### Electron Microscopy

The purified, lyophilized hemorrhagic fractions were dissolved in distilled water to give a final absorbance at 280 nm of 0.05 for HT*a*, 0.2 for HT*e*, and 0.4 for HT*b*. Experimental mice were injected with 0.1 ml of a sublethal dose of hemorrhagic toxin; control mice were injected with 0.1 ml of 0.85% physiologic saline (PSS). All mice were injected intramuscularly in the lateral aspect of the right thigh (biceps femoris muscle) and were killed by cervical dislocation at various times after injection of toxin or PSS. Muscle was taken

from the medial aspect of the injected thigh (gracilis and semimembranous muscles) to avoid sampling regions damaged by the needle. Eighty-two white mice weighing 18 to 20 g were used in eight experiments.

The tissue was fixed initially in 2% glutaraldehyde in cacodylate buffer (pH 7.4) for 2 hours at 4 C. After rinsing in three changes of the same buffer containing sucrose for 12 to 18 hours at 4 C, the tissue was postfixed in 2% osmium tetroxide in cacodylate buffer (pH 7.4) for 1 hour at 4 C. Dehydration through a graded series of ethanol was followed by embedment in Epon 812 [23] or Spurr [24] resin. After polymerization in a vacuum oven at 60 C for 48 hours, the blocks were sectioned on either a Sorvall MT-2 ultramicrotome or an LKB ultratome I with either glass or diamond knives. Thick sections (0.5 to 1.0 $\mu$) were cut, stained with toluidine blue,[25] and examined with the light microscope for areas of interest. Silver and silver-gray sections mounted on uncoated and unsupported copper grids were stained with 5% aqueous uranyl acetate and lead citrate [26] and were then observed and photographed with a Philips EM 200 electron microscope.

## Results

### Characteristics of Hemorrhagic Components

The characteristics of the three pure hemorrhagic components used in these experiments are listed in Table 1, which is a summary of data collected by Bjarnason [21] and Bjarnason and Tu.[14]

### Light Microscopic Observation

#### Control

No hemorrhage was observed either at the gross or light microscopic levels in control animals regardless of time between injection and death of the animal (1 minute to 3 hours) (Figure 1).

#### Experimental

Gross examination of muscle injected with hemorrhagic toxins *a* or *e* revealed ecchymotic hemorrhages at 2 minutes after injection; at 5 min-

Table 1—Characteristics of Hemorrhagic Toxins*

| Characteristic | Hemorrhagic toxin | | |
|---|---|---|---|
| | *a* | *b* | *e* |
| Molecular weight | 68,000 | 24,000 | 25,700 |
| Amino acid residues | 636 | 200 | 219 |
| Isoelectric point | Acidic | Basic | 5.6 |
| Zinc content (mole/mole) | 0.99 | 0.82 | 1.03 |
| Inhibited† by EDTA | + | + | + |
| Proteolytic‡ | + | + | + |

* Data taken from Bjarnason [21]

† Inhibition of hemorrhagic activity by EDTA is indicated by + .

‡ Presence of proteolytic activity is indicated by +.

utes the region of hemorrhage extended over the entire thigh. Light microscopic examination revealed varying degrees of damage depending on the interval between injection of the toxin and tissue sampling and on the distance of the area sampled from the center of hemorrhage.

*Hemorrhagic Toxin a.* Hemorrhagic toxin *a* produced extensive hemorrhage which was readily observed at the light microscopic level. In some regions the connective tissue was filled with erythrocytes, and broken vessels were observed (Figure 2).

*Hemorrhagic Toxin e.* Light microscopic examination of muscle injected with hemorrhagic toxin *e* revealed a connective tissue packed with erythrocytes and extruded plasma. The few intact capillaries were filled with erythrocytes and platelet aggregations (Figure 3).

*Hemorrhagic Toxin b.* Gross examination of muscle injected with hemorrhagic toxin *b* revealed no hemorrhage at 5 minutes, but there was a large hemorrhagic area over the thigh at 3 hours after injection. At the light microscopic level, interstitial edema was evident and the connective tissue was filled with extravasated erythrocytes. In some areas, few intact capillaries were observed and muscle necrosis was prominent (Figure 4). In these areas erythrocytes appeared to be located within damaged muscle cells. This is quite a contrast to the other toxins investigated since both hemorrhagic toxins *a* and *e* are hemorrhagic but not myotoxic.

### Electron Microscopy

#### Control

Capillaries in muscle from control animals conformed to the ultrastructure described previously.[27] The endothelium and underlying basal lamina were continuous. In the lumen there was a finely granular material, ie, plasma, and outside the capillaries were surrounded by collagen fibers and other connective tissue components. Endothelial cells contained nuclei of normal appearance with intact nuclear envelopes and areas of heterochromatin and euchromatin. The cytoplasm of endothelial cells contained numerous pinocytotic vesicles, small mitochondria, sparse endoplasmic reticulum (smooth and granular), and scattered ribosomes. Intercellular junctions were present and typical. Pericytes were often observed in their usual association with capillaries. Control skeletal muscle cells were also of normal structure. Collagen was prominent in the connective tissue and was of normal appearance (Figure 5).

#### Experimental

*Hemorrhagic Toxin a.* Hemorrhagic toxin *a* appeared to act directly on endothelial cells, resulting in lysis of their plasma membranes and leakage

of plasma and erythrocytes. The endothelium of affected vessels appeared to have become very thin prior to actual breakage (Figures 6 through 9). Gaps in the endothelium appeared to be within endothelial cells rather than between cells as indicated by the presence of intact intercellular junctions immediately adjacent to the openings (Figures 6, 8, and 9). In some vessels the endothelium was broken down into numerous small vesicles (Figure 7), which resulted again in gaps in the capillary wall. Fibrin was observed around some of the damaged capillaries (Figure 6). A common observation was the formation of platelet aggregations in damaged vessels especially at the site of endothelial rupture (Figure 8). Some of the platelets appeared to have undergone the platelet release action (Figures 8 and 9) as indicated by apparent loss of granules. Even in these vessels, intact intercellular junctions were present (Figures 8 and 9).

Collagen associated with damaged capillaries was usually disorganized, and the basal lamina was usually absent near and beneath ruptured endothelium (Figures 6 through 9).

The connective tissue surrounding damaged vessels was filled with a flocculant material, plasma, extravasated erythrocytes, and the normal connective tissue elements (Figures 6 and 8).

*Hemorrhagic Toxin b.* The pathogenesis of hemorrhage induced by hemorrhagic toxin *b* was very similar to that induced by toxin *a* except that it was much slower acting and it also caused necrosis of muscle. Toxin *b* caused endothelial cells to undergo a vesiculation (Figure 10) which resulted in gaps in the capillary wall through which blood escaped. Intercellular junctions adjacent to ruptured endothelium remained intact (Figure 10). Toxin *b* also caused marked necrosis of muscle (Figures 11 through 13) as indicated by the rupture of sarcolemma, breakdown of sarcoplasmic reticulum into numerous small vesicles, disoriented myofilaments, and abnormal mitochondria. Erythrocytes appeared to be located inside some damaged muscle cells (Figures 11 and 12). There was also an apparent increase in the amount of glycogen in ruptured muscle cells (Figure 13).

Mitochondrial changes in damaged muscle cells ranged from slight swelling to severe swelling and, most commonly, a stacking or reduplication of cristae (Figure 12). Numerous mitochondria of various shapes and sizes were observed in the connective tissue surrounding damaged muscle cells (Figure 13) and damaged capillaries (Figure 10).

*Hemorrhagic Toxin e.* Hemorrhagic toxin *e* acts rapidly to cause hemorrhage within 2 minutes after injection. It appeared to act on the endothelium to cause hemorrhage per rhexis. Endothelial cells became extremely thin and erythrocytes were observed passing through the thin portions of endothelial cell cytoplasm (Figures 14 and 15).

In some vessels swollen endothelial cells were seen adjacent to normal cells (Figures 15 and 16). This effect was accompanied by disruption of collagen and basal lamina (Figures 14 through 16), intravascular hemolysis (Figure 15), and slight swelling of muscle (Figure 16). There appeared to be some intravascular lysis of other blood cells, probably eosinophils from the morphology of the granules (Figure 15).

Many damaged vessels were plugged with platelet aggregations and the surrounding area was filled with a dense flocculant material and erythrocytes (Figure 16).

## Discussion

The intramuscular injection of crude rattlesnake (*C atrox*) venom causes degeneration of capillaries which results in hemorrhage by rhexis.[1] The pathogenesis includes initial swelling of endoplasmic reticulum, perinuclear space, and the entire endothelial cell. This is followed by rupture of the plasma membrane and extravasation of blood. Platelet aggregations plug gaps in vessel walls and often completely occlude the lumina. Since crude venom contains many varied components, it is difficult to ascribe these effects to any one of the components. By fractionating the venom and isolating pure hemorrhagic toxins, it is possible to study the pathogenesis of hemorrhage induced by a single known toxin. Bjarnason and Tu [14] reported the isolation of five hemorrhagic toxins from the venom of the Western Diamonback rattlesnake (*C atox*), and we are reporting here on the mode of action of three of these toxins. All three were found to be proteolytic. Toxin *a* has a molecular weight of 68,000 and is acidic; toxin *b* has a molecular weight of 24,000 and is basic; and toxin *e* has a molecular weight of 25,700 and is acidic (isoelectric point of 5.6).

All of the hemorrhagic toxins, HT*a*, HT*b*, and HT*e*, act directly on the capillary wall, causing degeneration of endothelial cells which results in rupture of their plasma membranes producing gaps through which blood escapes. These results confirm those reported by Ownby et al [1] using the crude venom of *C atrox*.

Only limited work has been done on the pathogenesis of hemorrhage induced by other crotalid venoms and their purified hemorrhagic toxins. Three hemorrhagic toxins (HR-1, HR-2a, and HR-2b) were isolated from the venom of the Habu snake (*T flavoviridis*). HR-2a and HR-2b were both shown to be free of proteinase activity using casein as a substrate [5] and they also lacked any hyaluronidase, phospholipase A, or collagenase activity. HR-1 was also found to be separable from proteolytic activity.[6] Yet all three components (HR-1, HR-2a, and HR-2b) plus collagenase liberated both proteins and carbohydrates from basement membrane [19] and their hemorrhagic activity was attributed to their ability to enzymat-

ically destroy the basement membrane and thus the stability of the capillary wall. Cinematographic and electron microscopic examination of tissue treated with HR-1 revealed that the toxin induced hemorrhage by diapedesis, the underlying cause being destruction of the basal lamina beneath the endothelium.[18] Electron microscopic examination of hemorrhage induced by the crude venom of the Habu snake showed that the mechanism of bleeding was also via the intercellular junctions.[28]

A nonproteolytic, acidic hemorrhagic toxin with molecular weight of 44,000 was isolated from the venom of *V palestinae*.[11] Subcutaneous injection of this toxin into rabbits resulted in the formation of gaps within endothelial cells and, thus, hemorrhage by rhexis.[29] These results agree with our results obtained using crude *C atrox* venom [1] (as well as the results reported here for the three hemorrhagic toxins HT*a*, HT*b*, and HT*e*) isolated from the same venom.

It appears that hemorrhage induced by crude crotalid venoms could be the result of two hemorrhagic mechanisms: hemorrhage by rhexis and hemorrhage by diapedesis. It also appears that although hemorrhage induced by purified hemorrhagic toxins may result from the two routes, the pathogenesis induced by the pure toxin(s) is the same as that induced by the crude venom from which it was extracted.

It is interesting to note that one of the hemorrhagic toxins from *C atrox* venom (HT*b*) also induced myonecrosis (see Figures 11 through 13). However, our study did not permit us to determine whether the myonecrosis was due to direct action of the toxin on muscle cells or to indirect action due to anoxia. The presence of necrotic muscle cells adjacent to intact capillaries (Figures 11 and 12) supports the idea that hemorrhagic toxin *b* (HT*b*) acts directly on the muscle cell. It is well established that myonecrosis occurs independently of vascular damage. We have shown that a pure component from *C viridis viridis* venom (myotoxin *a*) induces myonecrosis without any accompanying vascular lesions.[4] Thus, hemorrhagic toxin *b* could have a general effect on cell membranes; at least it acts on those of both skeletal muscle and endothelial cells.

## References

1. Ownby CL, Kainer RA, Tu AT: Pathogenesis of hemorrhage induced by rattlesnake venom: An electron microscopic study. Am J Pathol 76:401–414, 1974
2. Stringer JM, Kainer RA, Tu AT: Myonecrosis induced by rattlesnake venom: An electron microscopic study. Am J Pathol 67:127–140, 1972
3. Cameron DL, Tu AT: Characterization of myotoxin *a* from the venom of Prairie rattlesnake (*Crotalus viridis viridis*). Biochem 16:2546–2553, 1977
4. Ownby CL, Cameron D, Tu AT: Isolation of myotoxic component from rattlesnake (*Crotalus viridis viridis*) venom: Electron microscopic analysis of muscle damage. Am J Pathol 85:149–166, 1976

5. Takahashi T, Ohsaka A: Purification and some properties of two hemorrhagic principles (HR2a and HR2b) in the venom of *Trimeresurus flavoviridis:* Complete separation of the principles from proteolytic activity. Biochim Biophys Acta 207:65–75, 1970
6. Omori-Satoh T, Ohsaka A: Purification and some properties of hemorrhagic principle 1 in the venom of *Trimeresurus flavoviridis.* Biochim Biophys Acta 207:432–444, 1970
7. Ohsaka A, Takahashi T, Omori-Satoh T, Murata R: Purification and characterization of the hemorrhagic principles in the venom of *Trimeresurus flavoviridis.* Toxins of Animal and Plant Origin. Edited by A deVries, E Kochva. Vol 1. Lond, Gordon and Breach, 1971, pp 369–399
8. Omori T, Iwanaga S, Suzuki T: The relationship between the hemorrhagic and lethal activities of Japanese Mamushi (*Agkistrodon halys blomhoffii*) venom. Toxicon 2:1–4, 1964
9. Oshima G, Iwanaga S, Suzuki T: Studies on snake venoms. XVIII. An improved method for purification of the proteinase b from the venom of *Agkistrodon halys blomhoffii* and its physicochemical properties. J Biochem (Tokyo) 64:215–225, 1968
10. Oshima G, Omori-Satoh T, Iwanaga S, Suzuki T: Studies on snake venom hemorrhagic factor I (HR-I) in the venom of *Agkistrodon halys blomhoffii:* Its purification and biologic properties. J Biochem (Tokyo) 72:1483–1494, 1972
11. Grotto L, Moroz C, deVries A, Goldblum N: Isolation of *Vipera palestinae* hemorrhagin and distinction between its hemorrhagic and proteolytic activities. Biochim Biophys Acta 133:356–362, 1967
12. Mandelbaum FR, Reichl AP, Assakura MT: Some physical and biochemical characterisitcs of $HF_2$, one of the hemorrhagic factors in the venom of *Bothrops jararaca.* Toxicon 13:109, 1975
13. Nikai T, Sugihara H, Tanaka T: [Enzymochemical studies on snake venoms. II. Purification of lethal protein $Ac_1$-proteinase in the venom of *Agkistrodon acutus.*] J Pharmacol Soc Jpn 97:507–514, 1977
14. Bjarnason J, Tu AT: Hemorrhagic toxins from Western Diamonback Rattlesnake (*Crotalus atrox*) venom: Isolation and characterization of five toxins and the role of zinc in one of the toxins. Biochemistry (In press)
15. Sandbank U, Jerushalmy Z, Ben-David E, deVries A: Effect of *Echis coloratus* venom on brain vessels. Toxicon 12:267–271, 1974
16. McKay DG, Moroz C, deVries A, Csavossy I, Cruse V: The action of hemorrhagin and phospholipase derived from *Vipera palestinae* venom on the microcirculation. Lab Invest 22:387–399, 1970
17. Ohsaka A, Ohashi M, Tsuchiya M, Kamisaka Y, Fujishiro Y: Action of *Trimeresurus flavoviridis* venom on the microcirculatory system of rat: Dynamic aspects as revealed by cinephotomicrographic recording. Jpn J Med Sci Biol 24:34–39, 1971
18. Tsuchiya M, Ohshio C, Ohashi M, Ohsaka A, Suzuki K, Fujishiro Y: Cinematographic and electron microscopic analyses of the hemorrhage induced by the main hemorrhagic principle, HR1, isolated from the venom of *Trimeresurus flavoviridis.* Platelets, Thrombosis, and Inhibitors. Edited by P Didisheim, T Shimamato, H Yamazaki. Stuttgart, FK Schattauer, Verlag, 1974, pp 439–446
19. Ohsaka A, Just M, Habermann E: Action of snake venom hemorrhagic principles on isolated glomerular basement membrane. Biochim Biophys Acta 323:415–428, 1973
20. Hartree EF: Determination of protein: A modification of the Lowry method that gives a linear photometric response. Anal Biochem 48:422–427, 1972
21. Bjarnason J: Hemorrhagic toxins from the venom of *Crotalus atrox.* Doctoral thesis, Colorado State University, December, 1977
22. Kondo H, Kondo S, Ikezawa H, Murata R, Ohsaka A: Studies of the quantitative

method for determination of hemorrhagic activity of Habu venom. Jpn J Med Sci Biol 13:43–51, 1960
23. Luft JH: Improvements in epoxy resin embedding methods. J Biophys Biochem Cytol 9:409–414, 1961
24. Spurr AR: A low-viscosity epoxy resin embedding medium for electron microscopy. J Ultrastruct Res 26:31–43, 1969
25. Lynn JA: Rapid toluidine blue staining of Epon-embedded and mounted "adjacent" sections. Am J Clin Pathol 44:57–58, 1965
26. Venable JH, Coggeshall R: A simplified lead citrate stain for use in electron microscopy. J Cell Biol 25:407–408, 1965
27. Karnovsky MJ: Morphology of capillaries with special reference to muscle capillaries. Capillary Permeability. Edited by C Crone, NA Lassen. New York, Academic Press Inc., 1970, pp 341–350
28. Ohsaka A, Suzuki K, Ohashi M: The spurting of erythrocytes through junctions of the vascular endothelium treated with snake venom. Microvasc Res 10:208–213, 1975
29. McKay DG, Moroz C, deVries A, Csavossy I, Cruse V: The action of hemorrhagin and phospholipase derived from *Vipera palestinae* venom on the microcirculation. Lab Invest 22:387–399, 1970

## Acknowledgments

The authors would like to thank Jacque McArt and Lisa Seidman of the Electron Microscope Laboratory and Fred Lawson and Bill Glass of the Photography Laboratory at Oklahoma State University for their assistance and for making the labs available for use by the investigators.

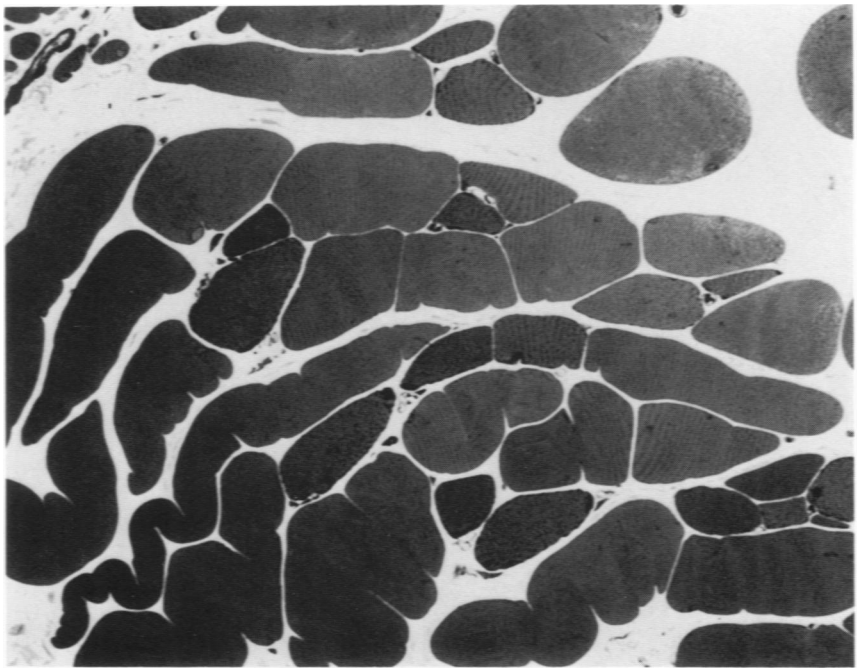

1

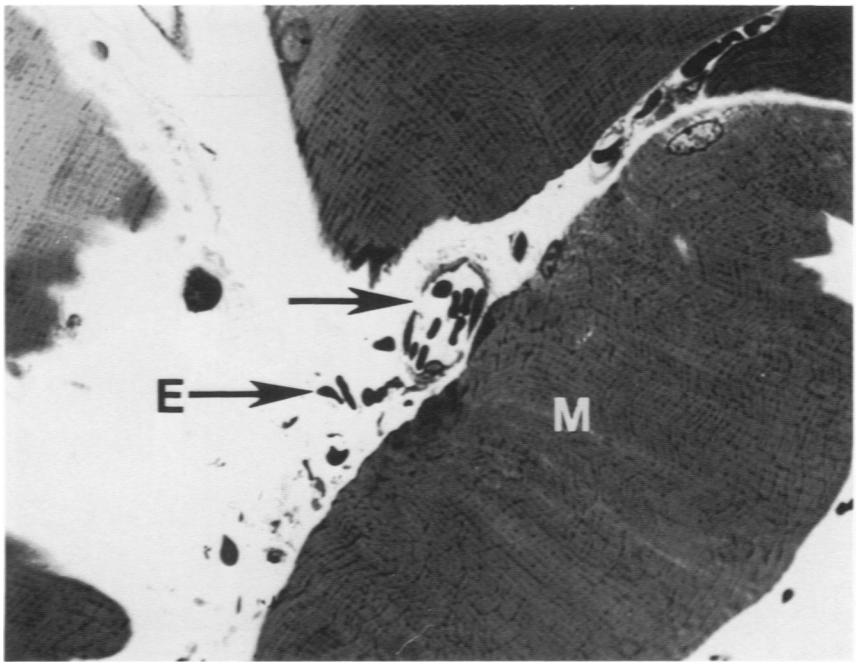


2

**Figure 1**—Light micrograph of control tissue. Capillaries are intact and the connective tissue is free of blood cells and plasma. (×250) **Figure 2**—Light micrograph of tissue 5 minutes after injection of hemorrhagic toxin *a* (HT*a*). *M*, muscle fiber. Note erythrocytes in connective tissue (*E*) and gap in vessel wall (*arrow*). (×700)

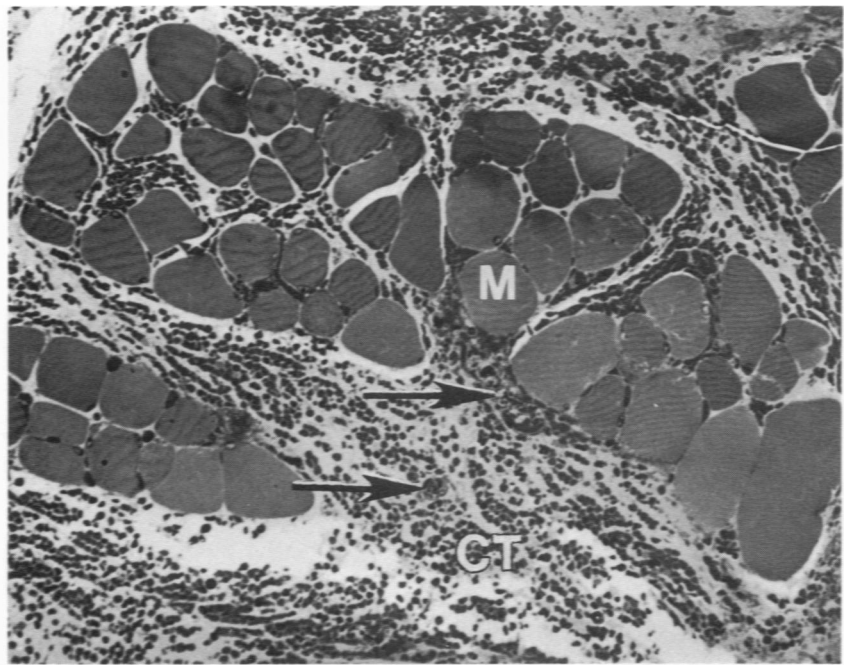


3

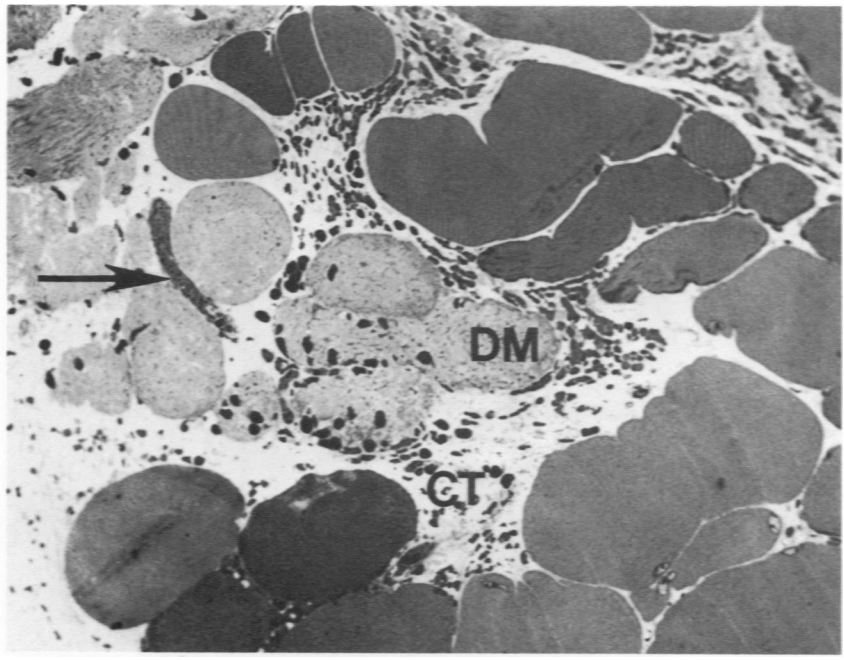


4

**Figure 3**—Light micrograph of tissue 5 minutes after injection of hemorrhagic toxin *e* (HT*e*). Muscle fibers (*M*) are normal in appearance, but the connective tissue (*CT*) is packed with extravasated blood. The few capillaries which are intact (*arrows*) appear to be packed with erythrocytes and platelets. (×300) **Figure 4**—Light micrograph of tissue 3 hours after injection of hemorrhagic toxin *b* (HT*b*). Note degenerating muscle cells (*DM*) which have lost their striated appearance and appear to contain erythrocytes. The connective tissue (*CT*) is filled with erythrocytes, and vessels (*arrow*) are packed with erythrocytes and platelets. (×600)

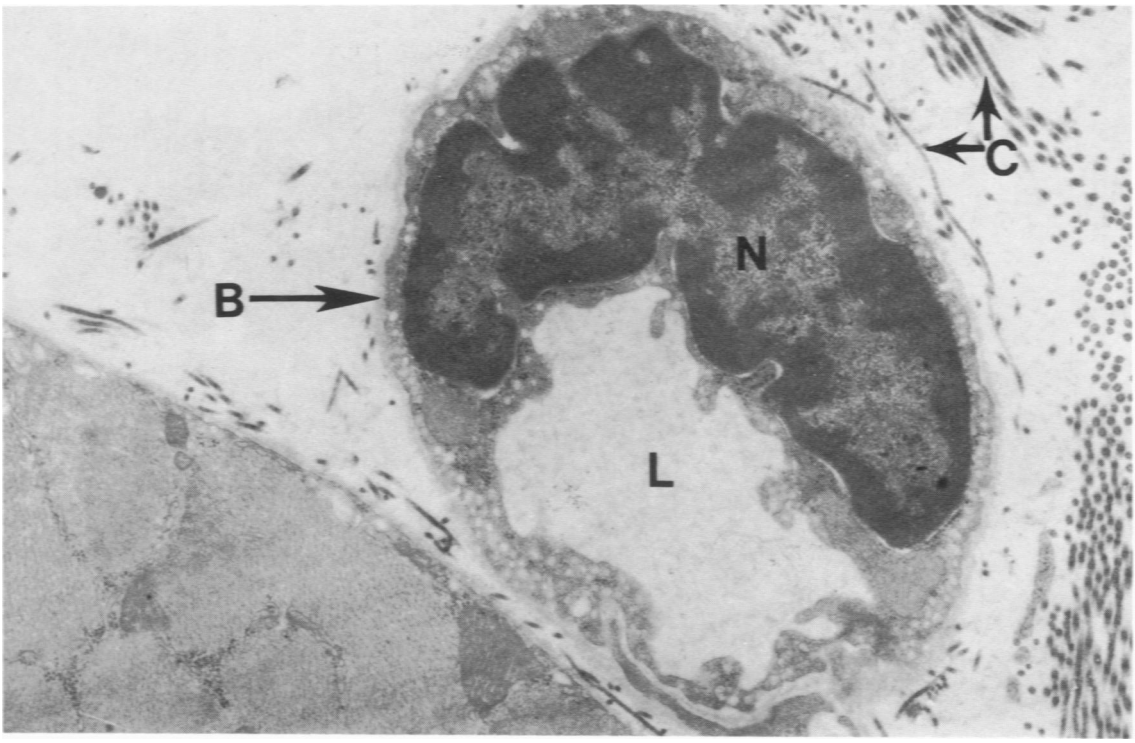


5

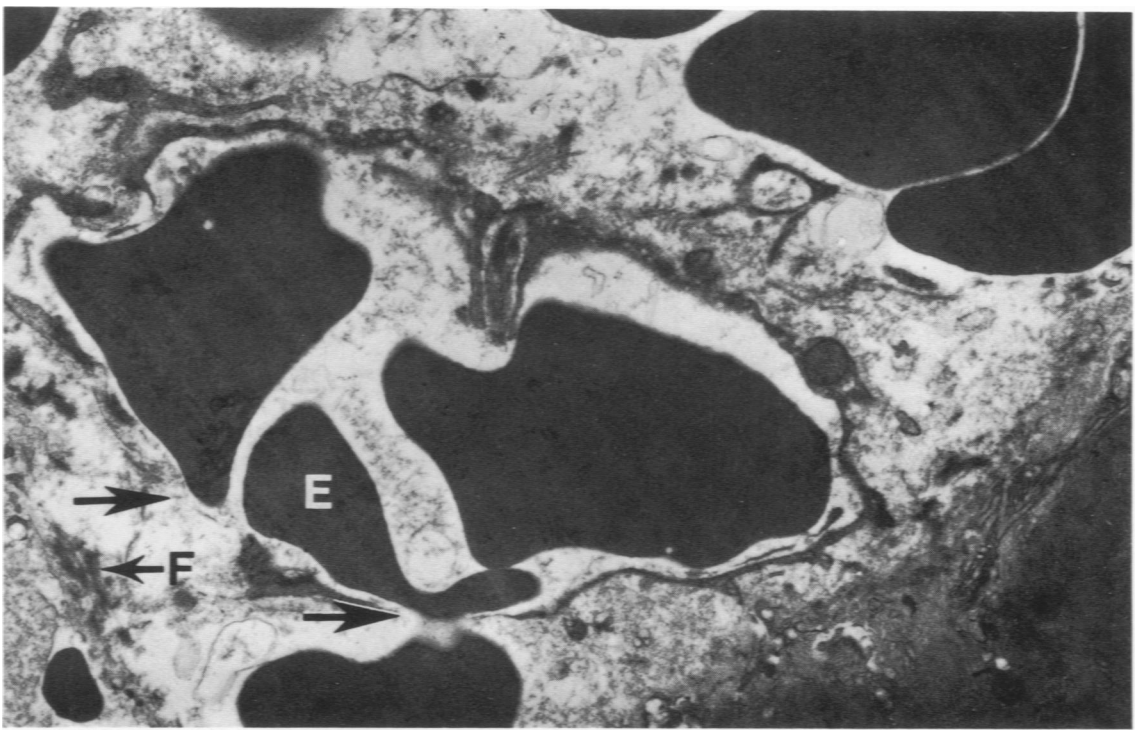


6

**Figure 5**—Electron micrograph of capillary from animal injected with physiologic saline. *N*, nucleus of endothelial cell; *L*, lumen; *C*, collagen; *B*, basal lamina. (×22,000)

**Figure 6 through 9** are electron micrographs of capillaries from animals injected with hemorrhagic toxin *a* (HT*a*).

**Figure 6**—Note thinness of endothelium and presence of large gaps (*arrows*) through which erythrocytes (*E*) are escaping. Note also the absence or disruption of collagen and the basal lamina (compare with Figure 5) and the presence of fibrin (*F*). (×17,500)

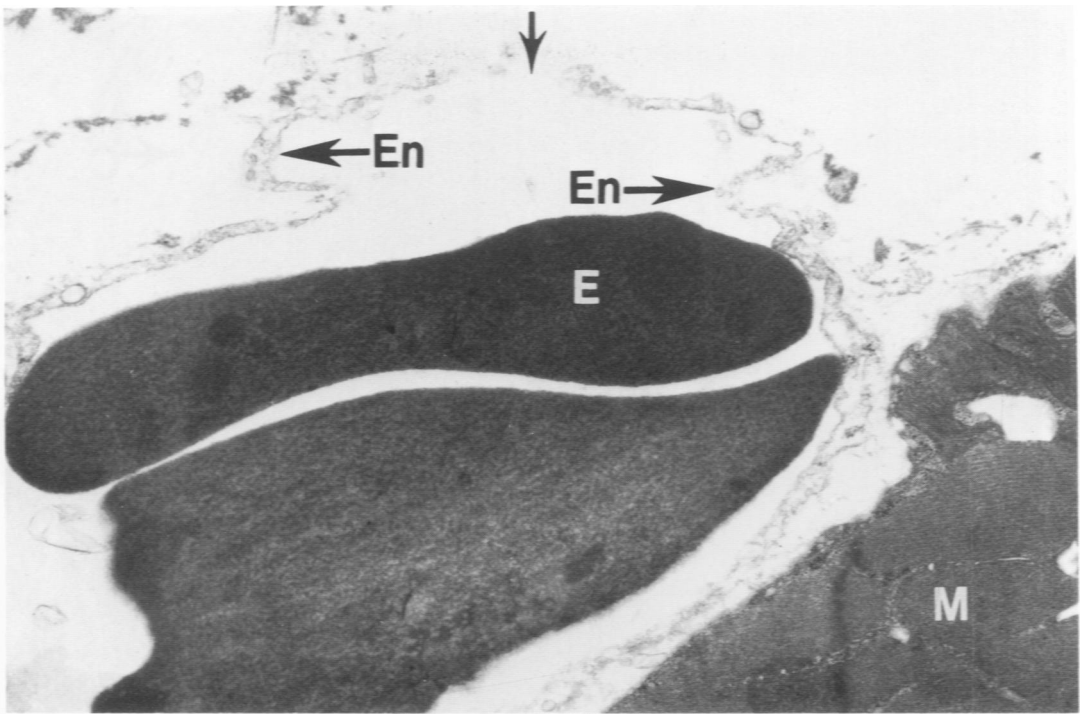


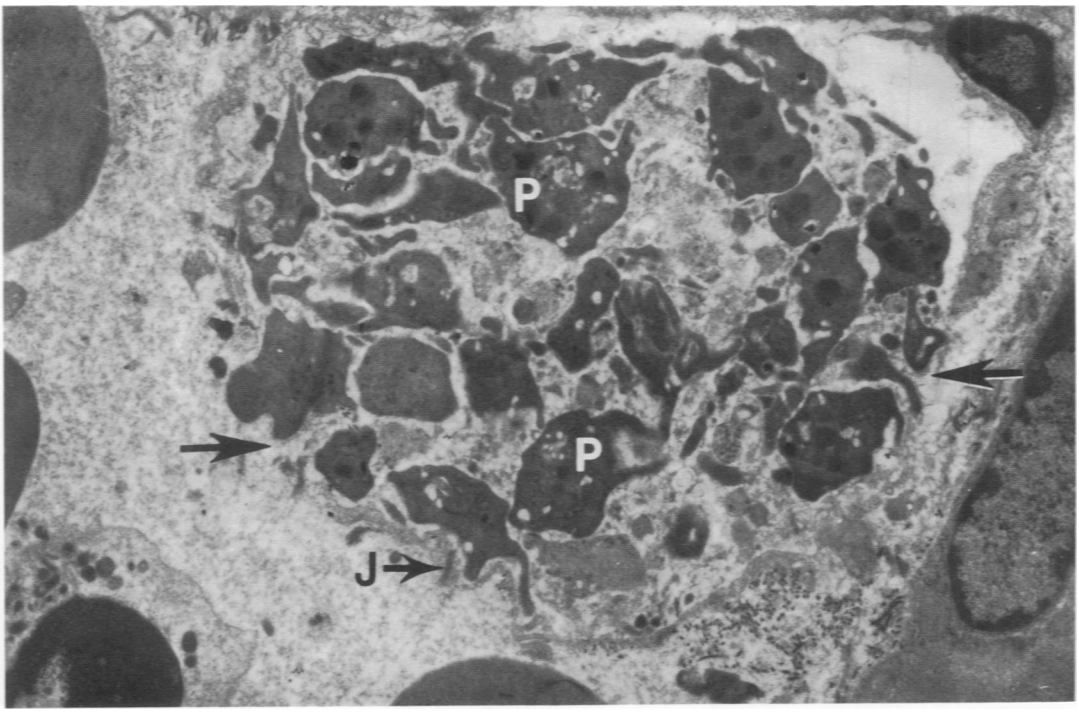


**Figure 7**—Note the very thin endothelium (*En*) and a gap in the vessel wall (*arrow*). *E*, erythrocyte; *M*, muscle. Also note the absence of collagen and basal lamina (compare with Figure 5). (×22,000)

**Figure 8**—This capillary is filled with a platelet aggregation (*P*). The endothelium is very thin and broken in several places (*arrows*). At least one intercellular junction is intact (*J*). (×13,000)

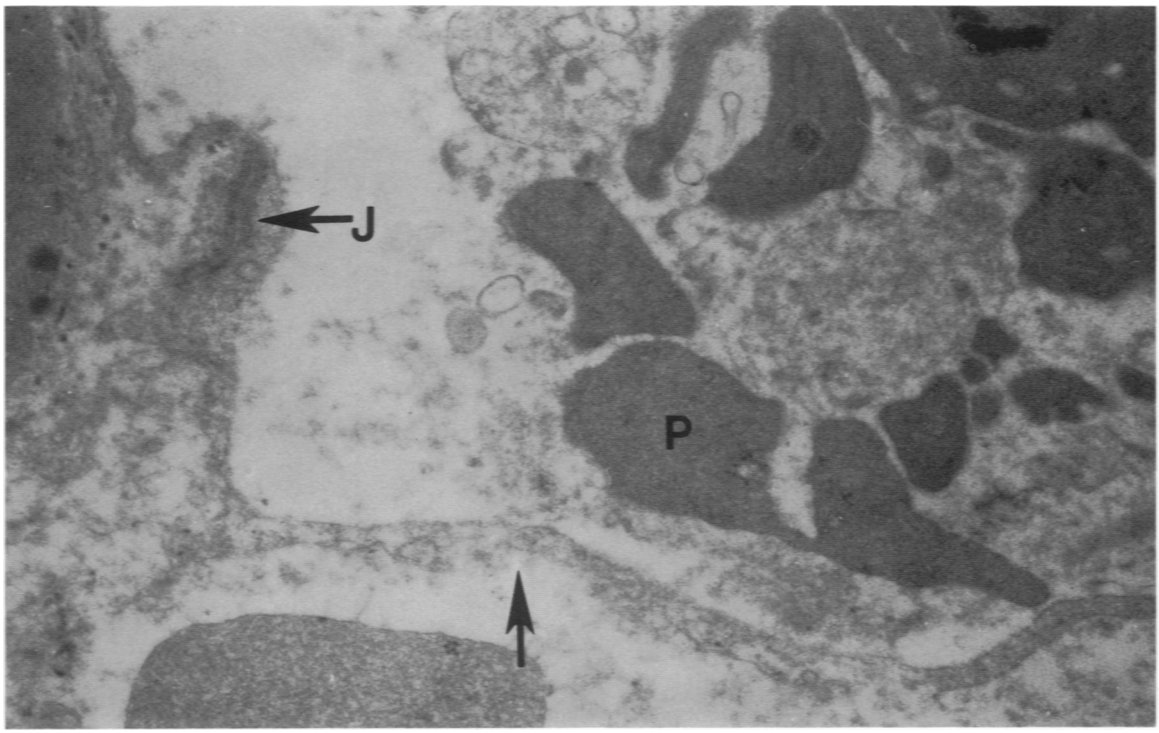


9

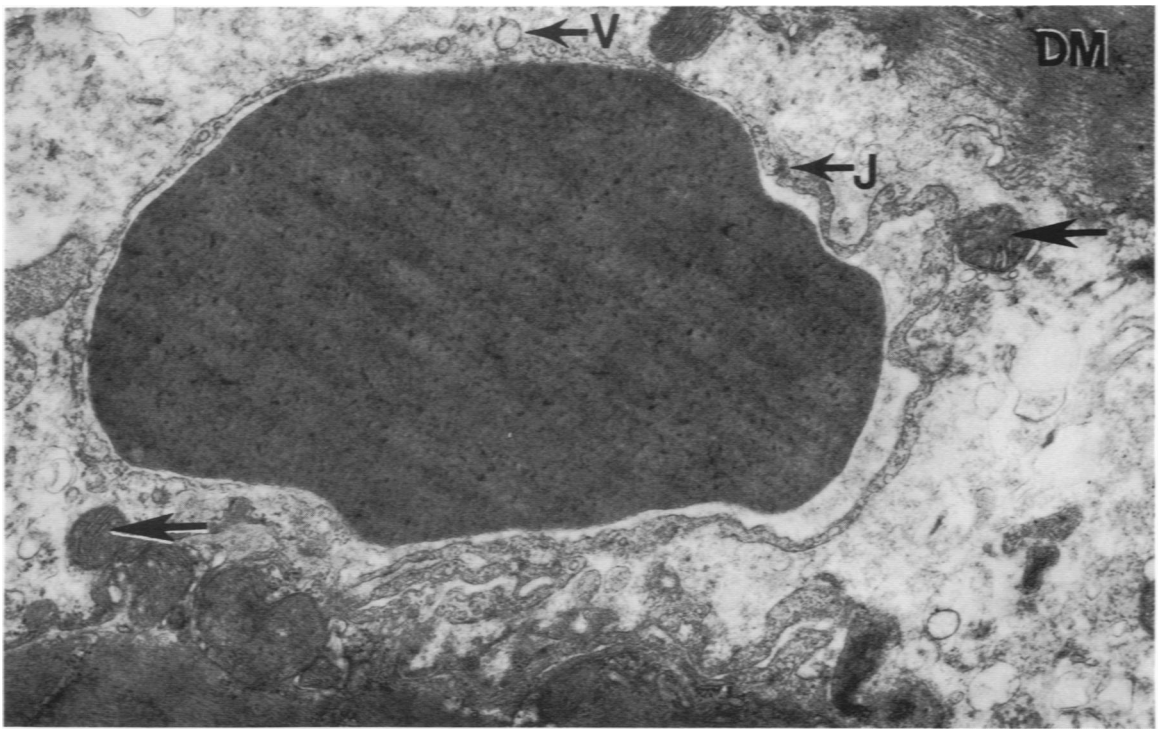


10

**Figure 9**—Higher magnification of a vessel similar to the one in Figure 8. Note the thin and broken endothelium (*arrow*), loss of collagen and basal lamina, presence of platelets (*P*), and intact intercellular junction (*J*). (×32,000) **Figures 10 through 13** are electron micrographs of capillaries and muscle from animals injected with hemorrhagic toxin *b* (HT*b*). **Figure 10**—Note vesiculation (*V*) of endothelium and presence of intact intercellular junction (*J*). Also note damaged muscle cell (*DM*) and free mitochondria (*arrows*). (×21,000)

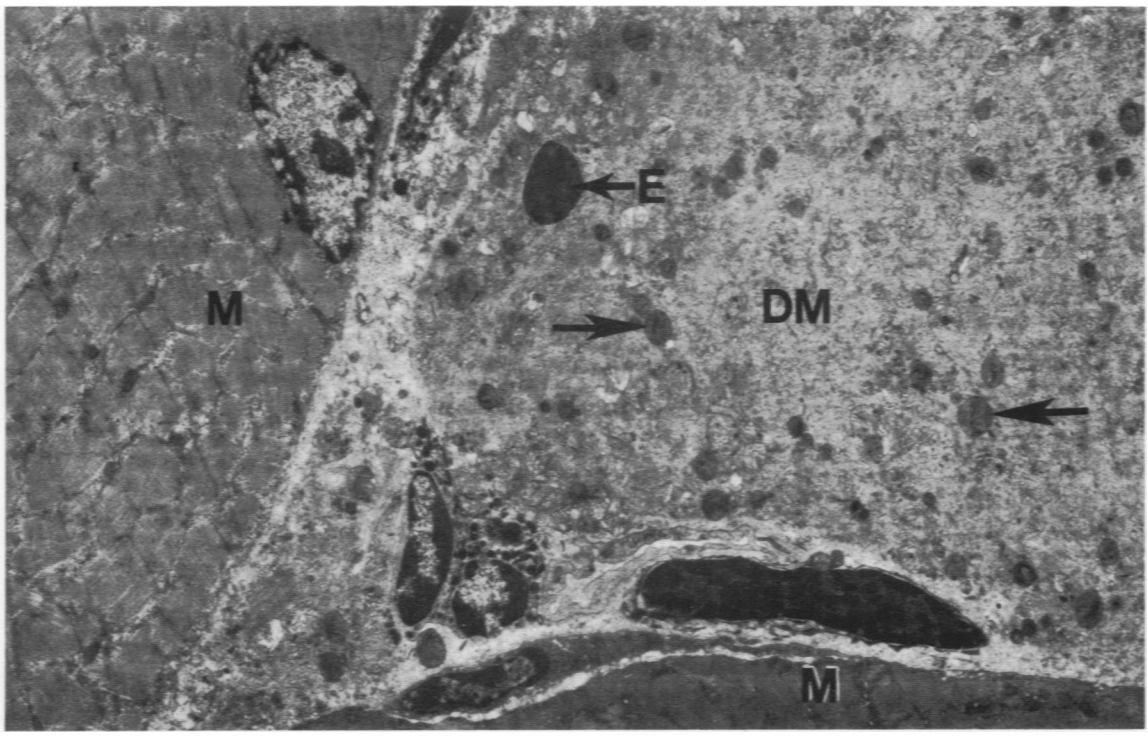


11

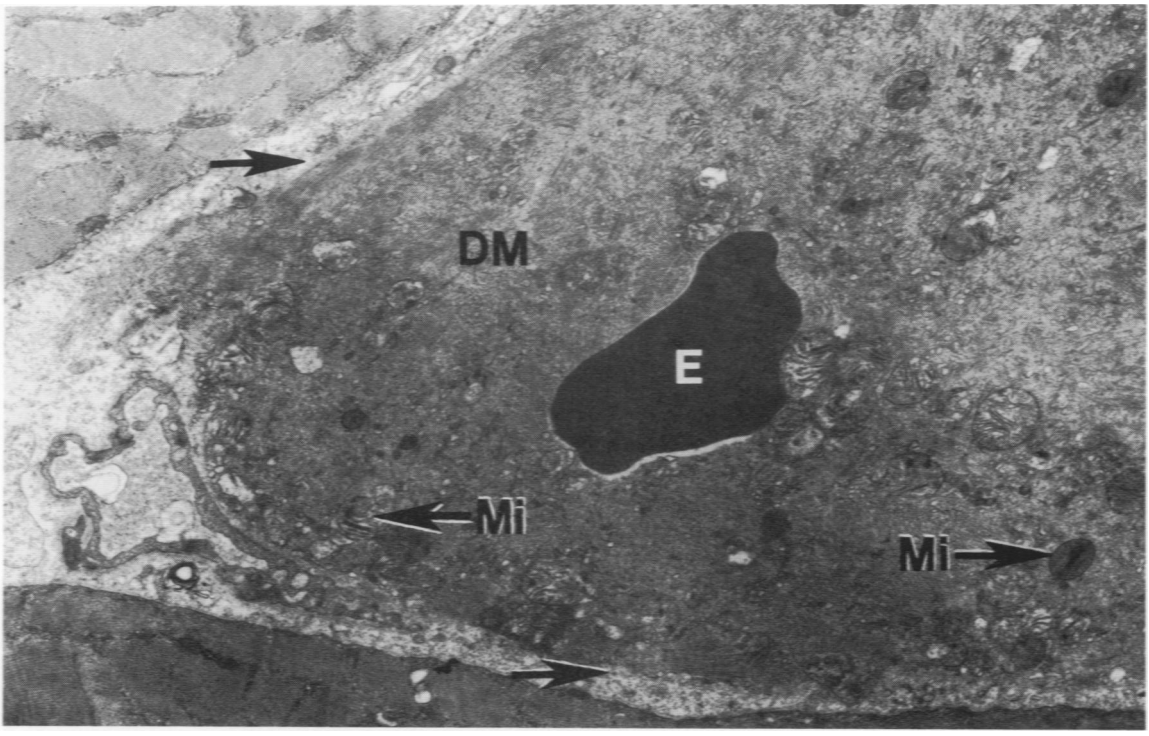


12

**Figure 11**—Note degenerating muscle cell (*DM*) and normal muscle cells (*M*). Also note erythrocyte (*E*) and abnormal mitochondria (*arrows*). (×6000) **Figure 12**—Note degenerating muscle cell (*DM*), erythrocyte (*E*), and mitochondria with reduplicated cristae (*Mi*). Also notice the absence of sarcolemma of necrotic muscle cell (*arrows*). (×10,000)

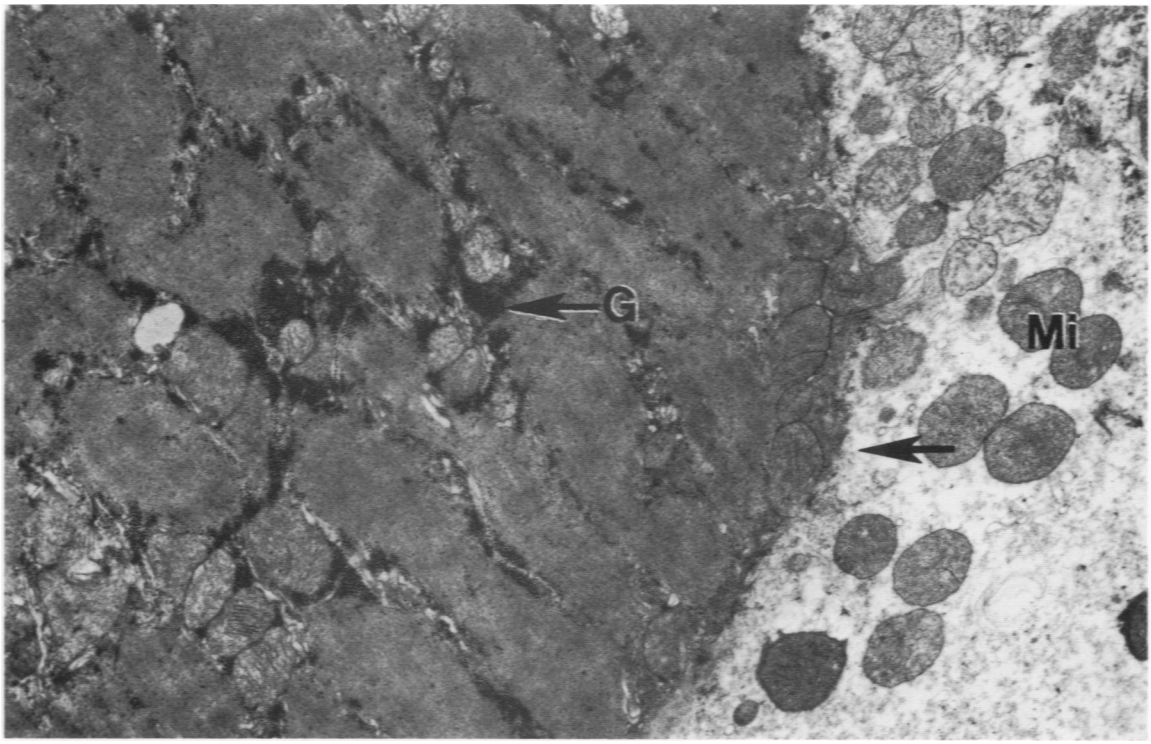


13

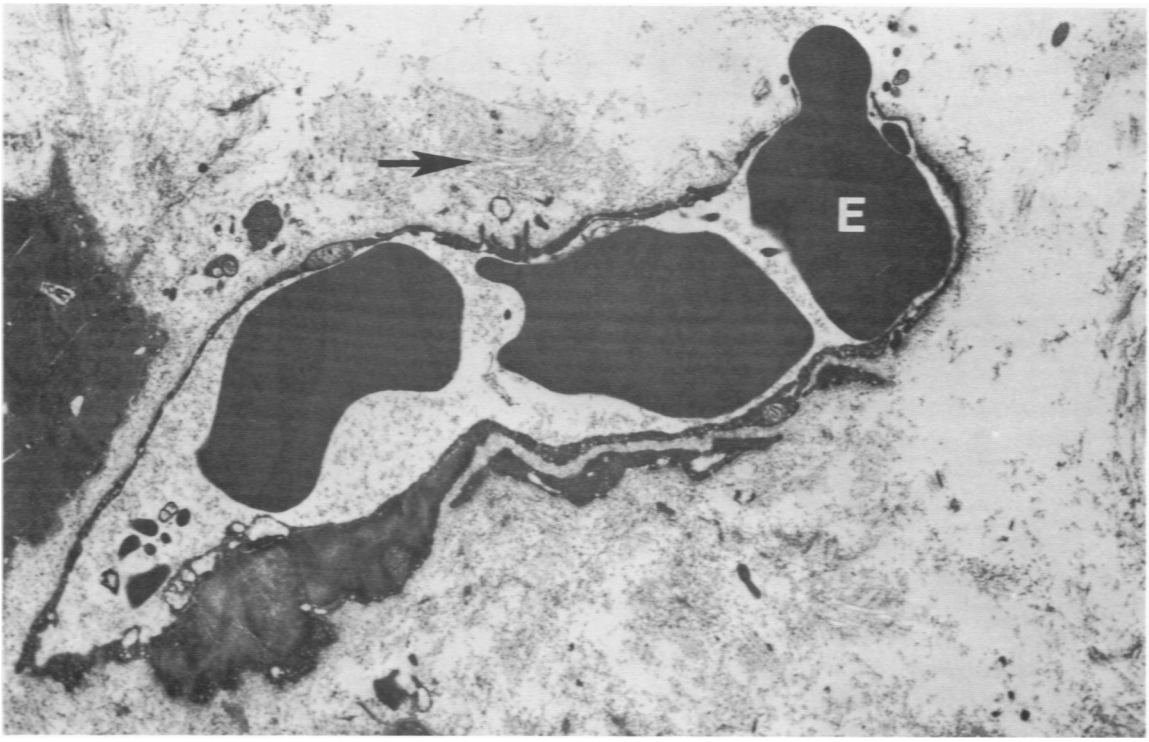


14

**Figure 13**—Muscle cell affected by HT*b*. Note lack of sarcolemma (*arrow*) and presence of mitochondria (*Mi*) in the endomysium. There appears to be an increase in glycogen (*G*) in the cell. (×13,000) **Figures 14 through 16** are electron micrographs of capillaries from animals injected with hemorrhagic toxin *e* (HT*e*). **Figure 14**—Erythrocyte (*E*) passing through a gap in endothelium. Note disruption of collagen beneath endothelium (*arrow*). (×10,500)

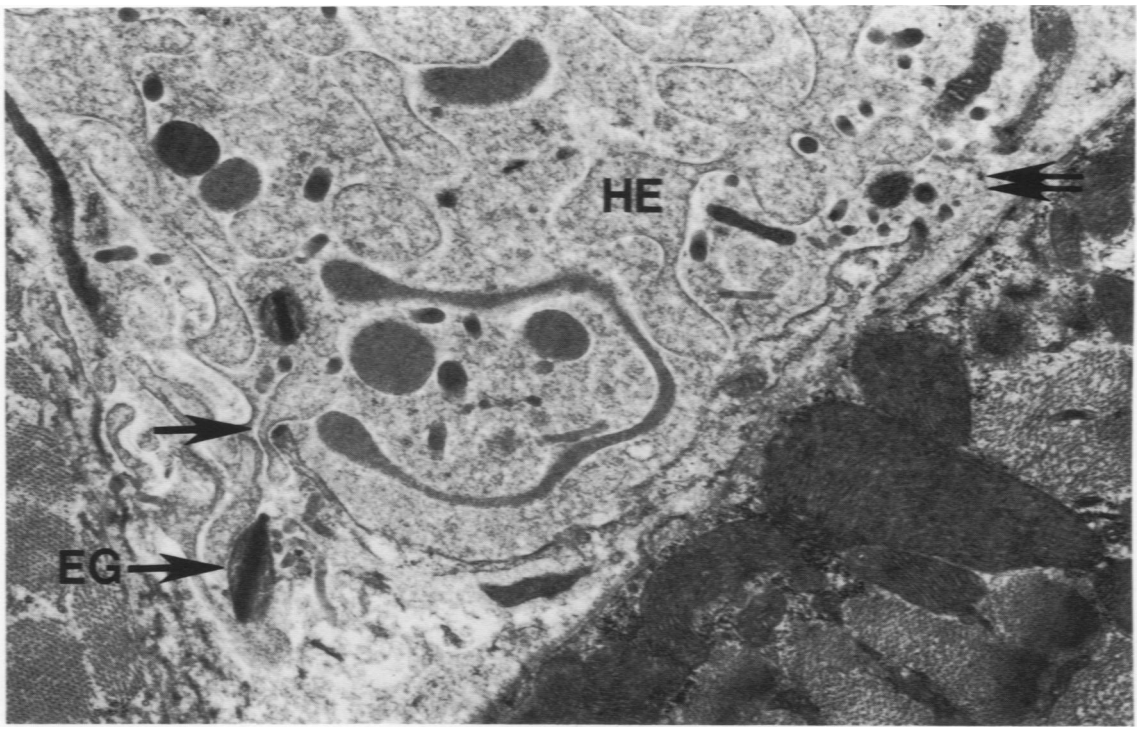


15

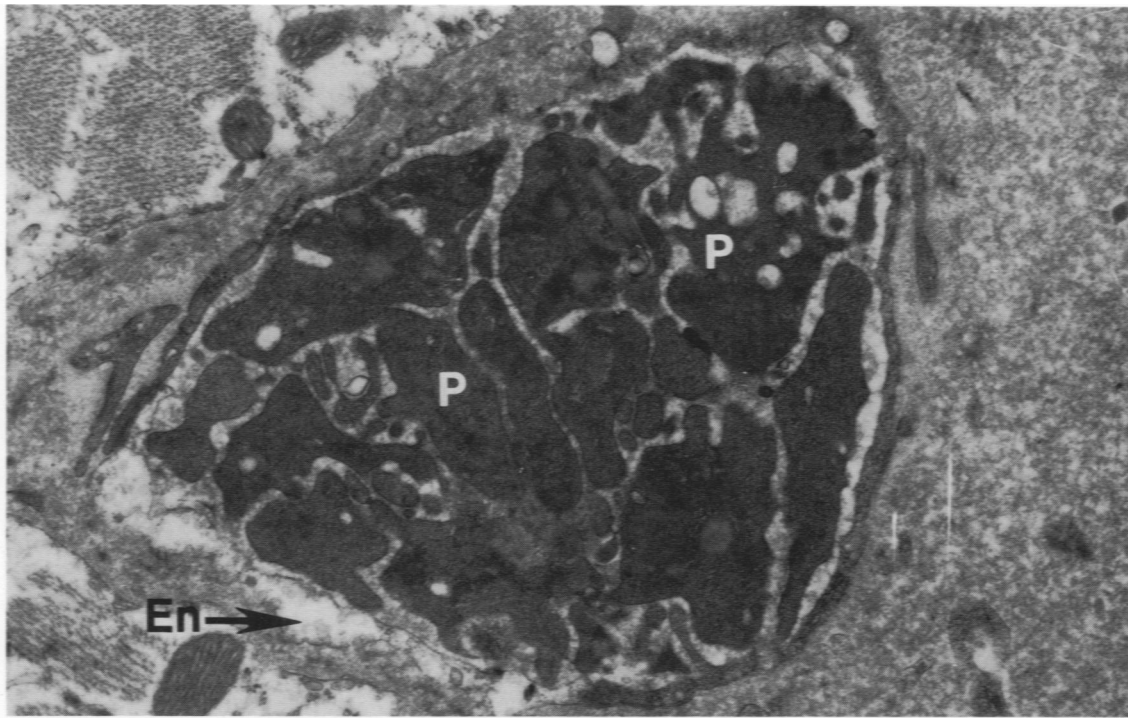


16

**Figure 15**—Note hemolyzed erythrocytes (*HE*) in the lumen and passing through a gap in vessel wall (*arrow*). It appears that granules from a lysed eosinophil (*EG*) are passing out through the same gap. Another gap is present in the same vessel (*double arrow*). Collagen fibers and the basal lamina are disrupted. (×22,000) **Figure 16**—Capillary filled with aggregation of platelets (*P*). Note flocculant material in connective tissue around vessel and swollen endothelial cell (*En*). (×22,000)